Journal of Photochemistry and Photobiology A: Chemistry 227 (2012) 45–50

Contents lists available at SciVerse ScienceDirect

Journal of Photochemistry and Photobiology A: Chemistry

journal homepage: www.elsevier.com/locate/jphotochem

Photodegradation of 2,4-D over $PdO/Al_2O_3–Nd_2O_3$ photocatalysts prepared by the sol–gel method

A. Barrera [a,*], F. Tzompantzi [b], V. Lara [b], R. Gómez [b]

[a] Universidad de Guadalajara, Centro Universitario de la Ciénega, Av. Universidad, Número 1115, Col. Linda Vista, Apdo. Postal 106, Ocotlan Jal., Mexico
[b] Universidad Autónoma Metropolitana – Iztapalapa., Departamento de Química, San Rafael Atlixco No. 186, Mexico 09340 D.F., Mexico

ARTICLE INFO

Article history:
Received 21 April 2011
Received in revised form 19 October 2011
Accepted 24 October 2011
Available online 11 November 2011

Keywords:
Photodegradation
2,4-D herbicide
$PdO/Al_2O_3–Nd_2O_3$ sol–gel
N_2 physisorption
XRD
UV–vis
FTIR

ABSTRACT

The photocatalytic activity of 1.0 wt% PdO supported on $Al_2O_3–Nd_2O_3$ binary oxides prepared by the sol–gel method was studied in the photodegradation of 2,4-dichlorophenoxyacetic acid (2,4-D). The photocatalysts were characterized by N_2 physisorption, XRD and UV–vis spectroscopy. PdO supported on γ-Al_2O_3 photo-degrades the 2,4-D, however the addition of Nd_2O_3 to γ-Al_2O_3 notably improves the photocatalytic activity. As the concentration of Nd_2O_3 in the binary oxide increases from 2 to 10 wt%, the photodegradation of 2,4-D is highly enhanced. The catalytic test for PdO supported on pure Nd_2O_3 showed scarce photocatalytic activity. Total organic carbon (TOC) analysis showed that the 2,4-D has been completely destroyed on the $PdO/Al_2O_3–Nd_2O_3$ photocatalysts after 6 h under irradiation.

1. Introduction

The intensive use of herbicides in agriculture frequently arises to the soil and water resources contamination [1]. Among them, the 2,4-dichlorophenoxyacetic acid (2,4-D) is the most commonly used herbicide in the world. This herbicide is widely applied in controlling broadleaf weeds in wheat, corn, rice, and similar cereal field crops. Generally the herbicide exhibits high persistency in soils, and on the surface and ground water effluents. The high hydro-solubility of the 2,4-D causes its mobility in the soil polluting through lixiviation underground water resources. This is especially important since water effluents can contaminate reservoirs of drinkable water. 2,4-D is a well known endocrine disrupter and affect the central and peripheral nervous system [2]. Therefore, the treatment of such pollutant compounds in water is highly required. Nowadays increased attention has been devoted to the application of photocatalysis as an advanced oxidation process for the elimination of organic pollutants in aqueous wastes using semiconductor materials as photocatalysts [3–6]. This approach is interesting since it allows the conversion of organic pollutants into harmless chemicals. Among these photocatalytic materials TiO_2 [7], ZnO doped TiO_2 [8,9], SnO_2 doped TiO_2 [10,11], layered double hydroxides [12–15], and Cr, Mn, Fe, Ni, Cu substituting metals in $CeVO_4$ [16] have been tested. In order to reach for highly active photocatalysts in the present work is reported the study of palladium oxide supported on alumina modified with rare earth oxides. It is known that palladium oxide (PdO) is a *p*-type semiconductor and it is of technological interest as a photocathode in water electrolysis [17]. However, to our knowledge the use of PdO supported on alumina as a photocatalyst for the degradation of herbicides has not been reported. Furthermore, it is reported that neodymium oxide can be used as doping agent for titania semiconductors for photocatalytic purposes [9,18–21] and it is the third more abundant element among lanthanides. With this in mind it should be very interesting to investigate the application of PdO supported on $Al_2O_3–Nd_2O_3$ binary oxides as a photocatalyst for the degradation of herbicides in aqueous milieu [2,7,8,22–24]. On the other hand, the physicochemical properties of the catalysts depend on the preparation method. Among the methods of synthesis, the application of the sol–gel method for the preparation of photocatalytic materials seems to be attractive, since it allows the preparation of homogeneous doped materials with high surface area and stability [9,25–29,10]. The $PdO/Al_2O_3–Nd_2O_3$ binary oxides prepared by the sol-method were characterized by N_2 physisorption, X-ray diffraction and

* Corresponding author. Tel.: +52 392 92 594 00; fax: +52 392 92 540 30.
E-mail addresses: arturobr@cuci.udg.mx (A. Barrera), fjtz@xanum.uam.mx (F. Tzompantzi).

1010-6030/$ – see front matter © 2011 Elsevier B.V. All rights reserved.
doi:10.1016/j.jphotochem.2011.10.023

UV–vis spectroscopy and were tested in the photodegradation of the 2,4-dichlorophenoxyacetic acid (2,4-D) herbicide.

2. Experimental

2.1. Synthesis of 1 wt% PdO catalysts supported on binary Al_2O_3–Nd_2O_3 oxides

Al_2O_3–Nd_2O_3 binary oxides (Al-Nd-*x*, where *x* = 2, 5, 10, and 100 wt% of Nd_2O_3) were synthesized by the sol–gel method as follows: aluminium tri-sec-butoxide, Al(O-SecBut.)$_3$ (Alfa Aesar) and Neodymium acetylacetonate, Nd(acac)$_3$.*x*H_2O (Alfa Aesar) were used as precursors. A required volume of aluminium tri-sec-butoxide was dissolved in a three mouth glass flask containing 10 mL of 2-methylpentane 2,4-diol (JT Baker) as a complexing agent at 70 °C and under stirring for 1 h. After cooling down to 50 °C, a required volume of a solution containing the neodymium acetylacetonate, dissolved previously in acetone at 40 °C for 1 h, was added into the three mouth glass flask containing the precursor solution. Then, the solution was heated with continuous stirring at 50 °C for 1 h until a transparent solution was formed. Afterwards, approximately 10 mL of deionised water were added to the solution drop by drop in order to carry out the aluminium alkoxide hydrolysis. The gels obtained were aged firstly at 55 °C for 2 h and then at 80 °C during 12 h. Samples were dried in an oven at 110 °C for 12 h followed by calcination under static air at 650 °C for 4 h. Pure Al_2O_3 (Al) was prepared by the same method as the mixed oxides but without the addition of lanthanum acetylacetonate. Pure Nd_2O_3 (Nd) was prepared by calcination of the neodymium acetylacetonate powder at 800 °C for 5 h. Al, Nd, and Al-Nd-*x* binary oxides samples, were impregnated with aqueous $PdCl_2$ (Aldrich) solution to obtain solids with 1.0 wt% PdO. The impregnated Al, Nd and Al-Nd-*x* binary oxide supports were dried in an oven at 110 °C for 12 h and then calcined in air at 650 °C for 3 h to give PdO/Al_2O_3 (PdO-A), PdO/Nd_2O_3 (PdO/Nd) and PdO/Al_2O_3–Nd_2O_3 (PdO/Al-Nd-*x*, where *x* = 2, 5, 10 wt% of Nd_2O_3) photocatalysts.

2.2. Characterization

The BET specific surface area (S_{BET}) of the PdO/Al_2O_3–Nd_2O_3 catalysts were determined on samples calcined at 650 °C for 3 h by nitrogen physisorption by using an Autosorb gas sorption system (from Quantachrome). Before measurements, samples were flushed with Ar at 200 °C for 2 h and then evacuated for 3 h at 200 °C.

X-ray powder diffraction patterns of the powder catalysts were recorded at room temperature with a Bruker D-8 Advance diffractometer with the Bragg–Brentano geometry, by using a Cu Kα (λ = 0.154 nm) radiation, a Ni 0.5% Cu-Kbeta-filter in the secondary beam, and a 1-dimensional position sensitive silicon strip detector (Bruker, Linxeye). The diffraction intensity as a function of the angle 2θ was measured between 20° and 110°, with a 2θ step of 0.01945°, for 53 s per point. Identification of the diffraction peaks from the XRD patterns was carried out by using the JCPDS database.

UV–vis diffuse reflectance spectra of calcined samples catalysts were recorded in a UV-Vis CARY 300 SCAN spectrometer with a scan speed of 600 nm min^{-1} with intervals of data collection of 1 nm and a change of the source light at a wavelength of 350 nm.

2.3. Photocatalytic degradation test

The photocatalytic activity test of the PdO/Al, PdO/Nd, and PdO/Al-Nd binary oxides were performed by using a batch-type cylindrical glass photoreactor of 1 L with a round bottom and surrounded by a double wall glass jacket. The herbicide used in the photodegradation experiments was 2,4 dichlorophenoxy acetic acid (2,4-D) (99.9%, Sigma–Aldrich). 80 mg of the 2,4-D herbicide were dissolved in 1 L of deionized water (0.362 mmol L^{-1}) and submitted to aeration during 2 h. A volume of 200 mL of the 2,4-D herbicide dissolution was put into the glass photoreactor followed by the addition of 200 mg of the photocatalyst to give a concentration of 1 mg of palladium photocatalyst per mL of 2,4-D herbicide solution. Then, the solution was submitted to continuous aeration (1 mL/s) and stirring until the photodegradation was initiated. A protected quartz tube with Pen-Ray UV power supply lamp (UVP products) with a typical wavelength of 254 nm and an intensity of 4400 μW cm^{-2} was immersed into the dissolution and used as the source of irradiation during the photodegradation experiments. Before irradiation, the 2,4-D solution and the catalyst were kept for 1 h without irradiation until the complete adsorption–desorption equilibrium of 2,4-D was reached on the solid. Then, the UV lamp was turned on. Samples of the irradiated dissolution were taken from the photoreactor and filtered each 2 h for a period of 6 h, in order to know the extent of photodegradation of the 2,4-D herbicide. The photodegradation of the 2,4-D herbicide was followed by UV–vis spectroscopy, employing a CARY 100 spectrophotometer with integration sphere. After ending the irradiation, the remaining 2,4-D–PdO/AlNd photocatalyst solids were dried at 80 °C for 12 h and then analyzed by FTIR spectroscopy using a PerkinElmer FT1730 spectrophotometer.

The evolution of the total organic carbon (TOC) during the photocatalytic runs was followed by using a TOC-V_{CEN} Shimadzu analyzer (catalytic oxidation on Pt at 680 °C). Calibration runs were performed by calibration curve of potassium phthalate.

Table 1
S_{BET} of PdO supported on Al_2O_3–Nd_2O_3 binary oxides.

Photocatalyst	S_{BET} (m^2 g^{-1})
1 wt%PdO/Al	180
1 wt%PdO/Al-Nd-2	242
1 wt%PdO/Al-Nd-5	248
1 wt%PdO/Al-Nd-10	259
1 wt%PdO/Nd	10

3. Results and discussion

3.1. Characterization of PdO catalysts supported on Al_2O_3–Nd_2O_3 binary oxides

Table 1 shows the S_{BET} of the various photocatalysts. The S_{BET} of the PdO/Al catalyst was 180 m^2 g^{-1}, whereas the S_{BET} for the PdO/Al-Nd-2, PdO/Al-Nd-5 and PdO/Al-Nd-10 catalysts were 242, 248 and 259 m^2 g^{-1} respectively. On the other hand, the S_{BET} of the PdO/Nd catalyst was 10 m^2 g^{-1}. The improvement in the S_{BET} of PdO/Al-Nd catalysts with the increase of the Nd_2O_3 content, suggests that the addition of Nd_2O_3 acts as a textural promoter of the γ-Al_2O_3 support. The presence of γ-Al_2O_3 in the binary oxide is corroborated by the XRD patterns (Fig. 1) where broad diffraction peaks at 2θ = 19.4, 37.5, 39.6, 45.9, 60.5 and 66.8 belonging to the (1 1 1), (3 1 1), (2 2 2), (4 0 0), (5 1 1) and (4 4 0) planes of the γ-Al_2O_3 phase (29–63, 10–425 JCPDS) can be seen. In addition, some diffraction peaks at 2θ = 33.98 and 54.95 belonging to the (1 0 1) and (1 1 2) planes of the tetragonal PdO phase (00-041-1107 JCPDS) are also observed in the XRD patterns. This suggests the presence of big PdO crystallites in the palladium catalysts supported on the Al_2O_3–Nd_2O_3 binary oxides. When the Nd_2O_3 content in the Al_2O_3–Nd_2O_3 binary oxide is 2 wt% (PdO/Al-Nd-2), the XRD pattern is almost similar to that of the PdO/Al sample. At higher Nd_2O_3 concentration, a decrease in the intensity as well as the widening of the Al_2O_3 diffraction peaks are observed in the XRD patterns suggesting a decrease in the γ-Al_2O_3 crystallite size. These results

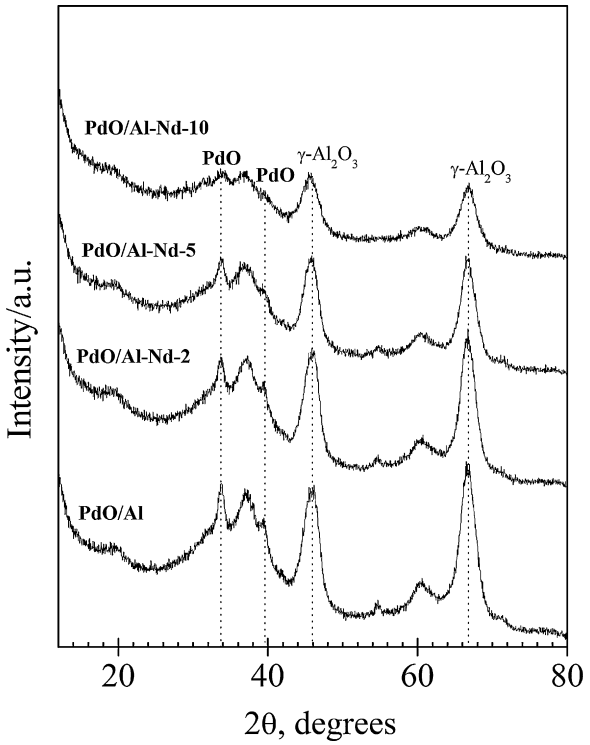

Fig. 1. X-ray diffraction patterns of 1 wt% PdO supported on Al_2O_3–Nd_2O_3 binary oxides.

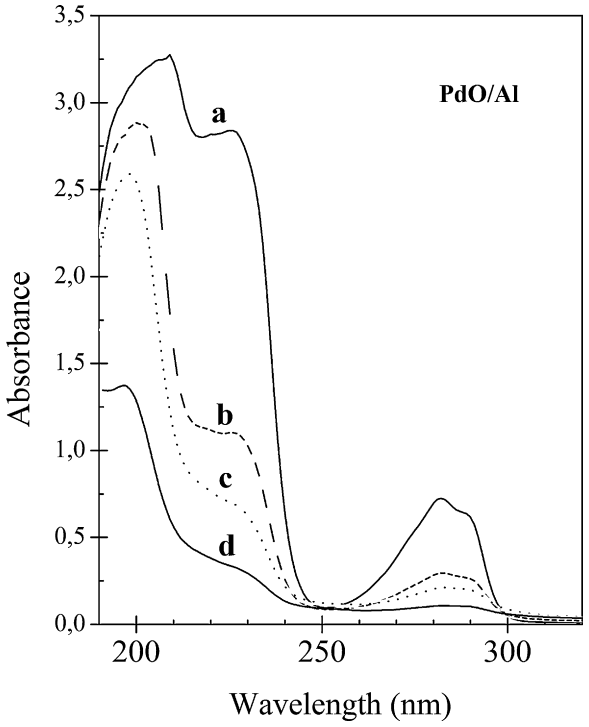

Fig. 3. UV spectra for the photodegradation of the 2,4-D over 1 wt%PdO/Al_2O_3 catalyst after: (a) 0 h; (b) 2 h; (c) 4 h; and (d) 6 h of irradiation.

justify the increase in the BET specific surface area for the samples containing 2.0, 5.0 and 10 wt% Nd_2O_3 on the binary oxide.

In Fig. 2 the UV–vis spectra of palladium oxide supported on Al_2O_3, Al_2O_3–Nd_2O_3 binary oxides, and Nd_2O_3 are presented. For the PdO/Al catalyst an absorption band at ca. 212 nm and an absorption edge in the visible region between 490 and 600 nm can be seen. The band at ca. 212 nm is assigned to Pd^{2+} states of highly dispersed PdO particles [30,31]. Whereas, the absorption edge between 490 and 600 nm belongs to the semiconductive electronic structure of crystalline PdO [31]. UV–vis spectra of PdO/Al-Nd catalysts show the same absorption bands for the PdO/Al-Nd-2 and PdO/Al catalysts. For the PdO/Al-Nd-5 and PdO/Al-Nd-10 samples, however new absorption bands can be seen 580, and 744 nm. It is well known that UV–vis spectroscopy reveals the influence of crystal field on the electronic transitions in *f* orbitals of the rare earth elements [32,33]. By comparing the absorption bands of the UV–vis spectra of PdO/Al-Nd catalysts with those of PdO/Nd catalyst we infer that they correspond to Nd^{3+} transitions. However, the more intense and sharp absorption bands observed at ca. 592 and 750 nm in the UV–vis spectra of the PdO/Nd catalyst are slightly shifted to a lower wavelength for about 13 nm in the UV–vis spectra of the PdO/Al-Nd catalysts. This shifting in the absorption bands could be related to the modification in the coordination sphere of Nd^{3+} cations due to interaction with Al^{3+} cations. In fact, Caro [33], reported the shift of the $^4I_{9/2}$–$^2P_{1/2}$ transition of the $4f^3$ orbital between Nd^{3+} in Nd_2O_3 and the same ion in $NdAlO_3$ with a perovskite structure. The interaction between Al^{3+} and Nd^{3+} cations could be facilitated by the sol–gel preparation route due to that the compounds in the materials are homogenously well mixed arising to a higher interaction and an easier inter-diffusion between species.

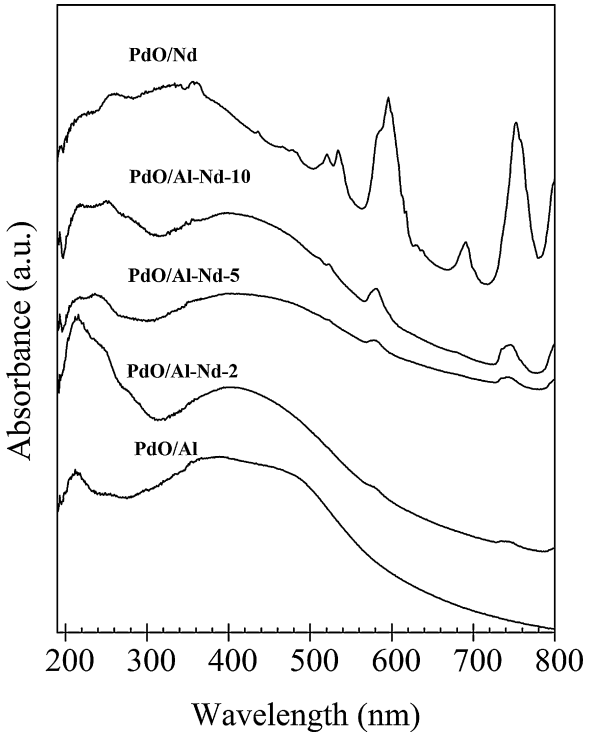

Fig. 2. UV–vis spectra of 1 wt% PdO photocatalysts supported on Al_2O_3–Nd_2O_3 binary oxides.

3.2. Photodegradation of the 2,4-D herbicide

Fig. 3 shows the photocatalytic activity of PdO/Al catalyst in the photodegradation of the 2,4-D herbicide. This figure shows that the intensity of the absorption band at 200 nm belonging to the electronic transition $\pi \rightarrow \pi^*$ of the aromatic groups decreases with time under irradiation indicating the elimination of aromatic molecules in the solution, another absorption band at 270 nm indicates the decomposition of benzene functional groups. The PdO/Al

Table 2
Conversion % of aromatic groups in the photodegradation of 2,4-D over PdO photocatalysts supported on Al_2O_3–Nd_2O_3 binary oxides.

Irradiation time (h)	Conversion % of aromatic groups photocatalysts				
	PdO/Al	PdO/Al-Nd-2	PdO/Al-Nd-5	PdO/Al-Nd-10	PdO/Nd
2	8	17	19	38	1
4	18	38	50	80	6
6	59	70	86	95	22

photocatalyst eliminates about 8%, 18% and 59% of the aromatic groups after 2, 4 and 6 h of irradiation respectively (Table 2). When 2 wt% of neodymium oxide is added to γ-Al_2O_3 by the sol–gel method the photocatalytic activity of the PdO/Al-Nd-2 photocatalyst (Fig. 4) improves to 17%, 38% and 70% of elimination of aromatic groups after the same times of irradiation respectively. The improvement in the photocatalytic activity is also observed in the PdO/Al-Nd-5 and PdO/Al-Nd-10 photocatalysts (Table 2 and Fig. 5) compared to PdO/Al photocatalyst. The photocatalytic activity in the photodegradation of the 2,4-D increases as the concentration of Nd_2O_3 in the binary oxide support increases to 10 wt% (Table 2). The less active photocatalyst was the PdO supported on pure Nd_2O_3 (Fig. 6) since it converts only 22% of aromatic groups of 2,4-D after 6 h of irradiation. The lower photodegradation of aromatics groups observed with PdO/Nd is correlated with its lowest S_{BET}. It suggests that the nature of the support and thereby the chemical state of neodymium oxide is crucial in order to promote the activity of PdO/Al catalysts for the photodegradation of the 2,4-D in aqueous milieu. It means that at least 2 wt% of neodymium oxide added to γ-Al_2O_3 is needed in order to promote the photodegradation of 2,4-D.

Figs. 7 and 8 show that the 2,4-D herbicide is strongly adsorbed on the photocatalysts surface establishing the equilibrium after one hour of adsorption. However, when the UV irradiation was turned on, a continuous decrease in the concentration of the solution was observed degrading more than 90% of 2,4-D herbicide after

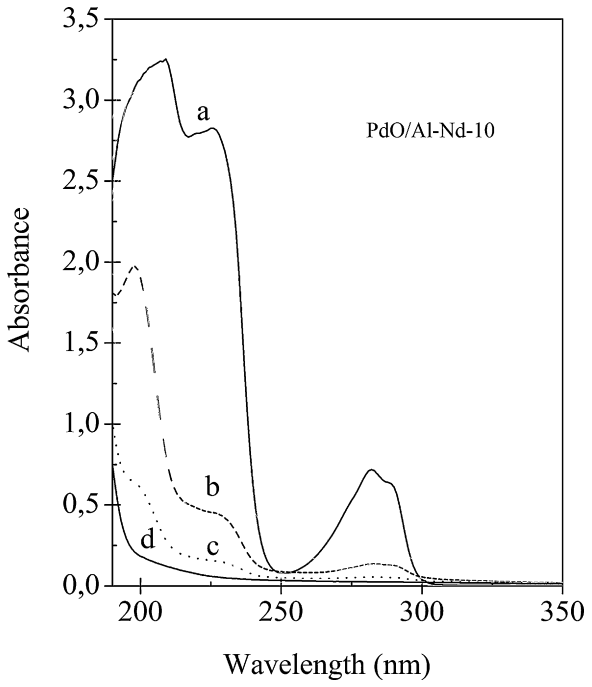

Fig. 5. UV spectra of the photodegradation of the 2,4-D over the 1 wt%PdO/Al-Nd-10 photocatalyst after: (a) 0 h; (b) 2 h; (c) 4 h; and (d) 6 h of irradiation.

6 h of irradiation. An increase in the Nd_2O_3 concentration in the Al_2O_3–Nd_2O_3 binary oxides showed an apparent increase of the capability of adsorption and photodegradation of the 2,4-D. It is noteworthy to point out that due to the strong adsorption of the 2,4-D, it was not possible to calculate a correct kinetics of the photocatalytic degradation in aqueous solution, reason for which were carried out studies of the solution during the process of photodegradation and also studies of the solids by FTIR spectroscopy in order

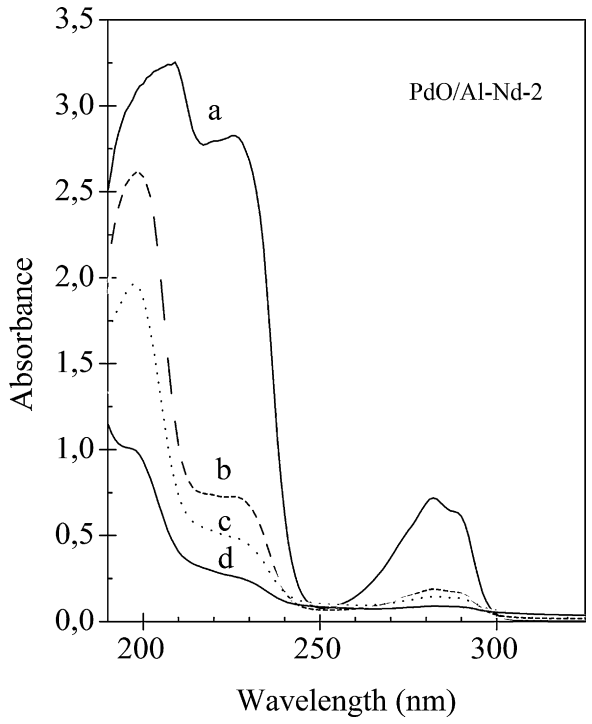

Fig. 4. UV spectra of the photodegradation of the 2,4-D over 1 wt%PdO/Al-Nd-2 photocatalyst after: (a) 0 h; (b) 2 h; (c) 4 h; and (d) 6 h of irradiation.

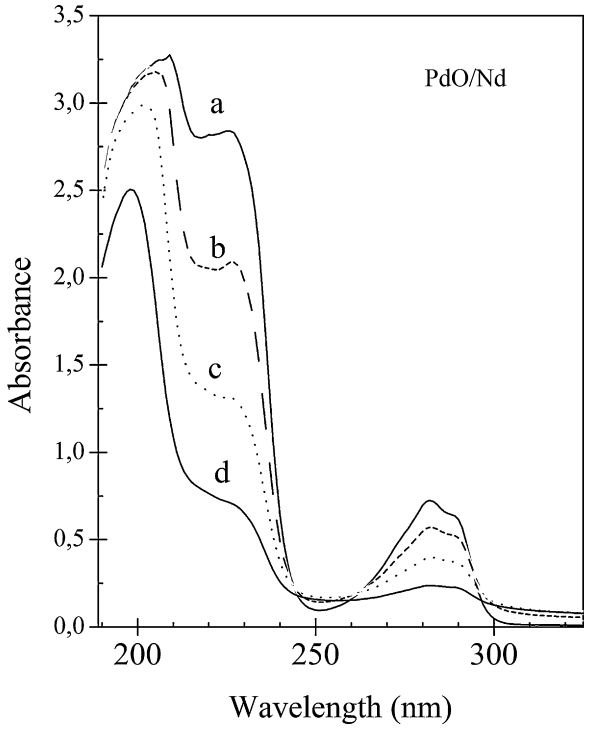

Fig. 6. UV spectra of the photodegradation of 2,4-D over 1 wt%PdO/Nd_2O_3 photocatalyst after: (a) 0 h; (b) 2 h; (c) 4 h; and (d) 6 h of irradiation.

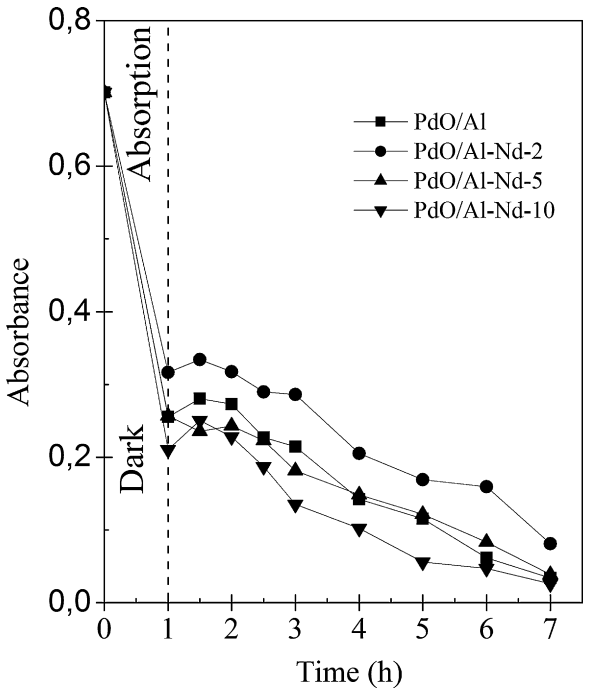

Fig. 7. Evolution as a function of time under irradiation for the 2,4-D degradation on 1 wt% PdO supported on Al_2O_3–Nd_2O_3 binary oxides.

to corroborate the total elimination of the 2,4-D. Furthermore, total organic carbon analysis (TOC) during the photocatalytic runs were carried out in order to analyze the amount of the organic compound eliminated.

The FTIR spectra of the recovered solids after irradiation of the (2,4-D-PdO/Al-Nd) photocatalyst are shown in Fig. 9. The FTIR spectra for the 2,4-D solution without photocatalyst before irradiation is showed. In this spectra typical absorbance bands at ca. 1092, 1106, 1233, 1309, 1477, and 1733 cm^{-1} assigned to the

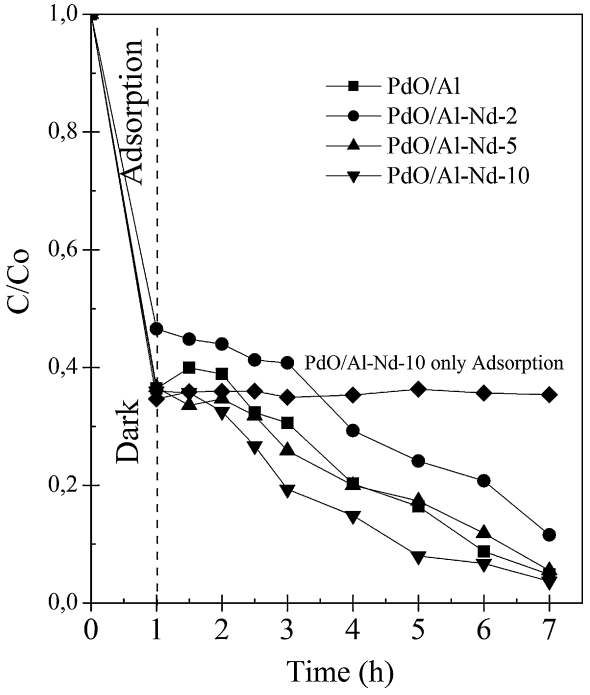

Fig. 8. Relative concentration (C/C_0) of the 2,4-D as a function of time under irradiation on 1 wt% PdO supported on Al_2O_3–Nd_2O_3 binary oxide.

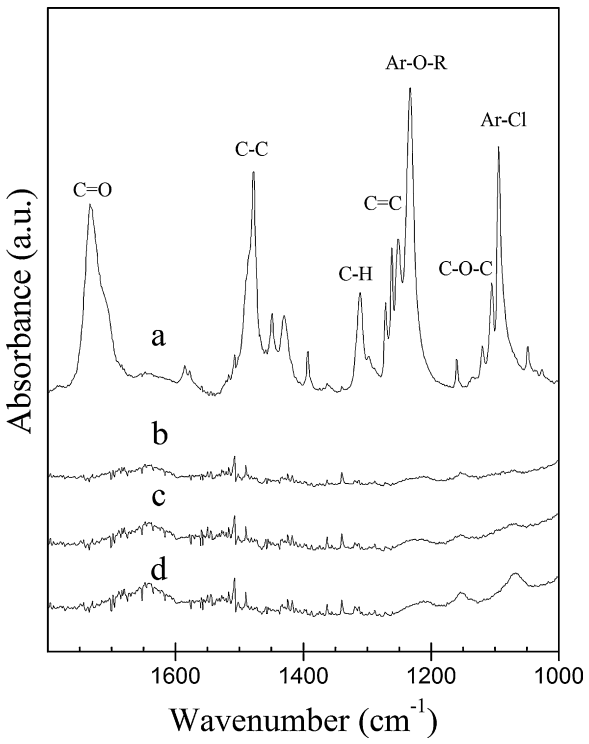

Fig. 9. FTIR of the 2,4-D herbicide and 1 wt% PdO supported on Al_2O_3–Nd_2O_3 binary oxides: (a): 2,4-D solution; (b): PdO/Al-Nd-2; (c): PdO/Al-Nd-5; and (d): PdO/Al-Nd-10 recovered catalysts from the 2,4-D solution after 6 h under irradiation.

stretching vibrations bands of the ν(Ar–Cl), ν(C–O–C), ν(Ar–O–R), ν(C–H), ν(C–C), and ν(C=O) functional groups of 2,4-D can be seen, while the FTIR spectra of the recovered photocatalysts after irradiation do not show the presence of 2,4-D functional groups. It can be assumed that the 2,4-D molecule have been completely destroyed by the PdO/Al-Nd photocatalysts after 6 h of irradiation since their spectra do not show any absorption bands belonging to the characteristic vibrations of the stretching mode of the 2,4-D molecule.

The total organic carbon analysis (TOC) of the irradiated 2,4-D solutions is showed in Fig. 10. It is observed that approximately 40% of the 2,4-D molecules are adsorbed on the photocatalysts surface without irradiation as shown for the PdO/Al-Nd-10 photocatalyst. When the photodegradation is started the increase in the Nd_2O_3 content in the Al_2O_3–Nd_2O_3 binary oxides favors the efficiency for the elimination of 2,4-D. A residual concentration TOC (at ca. 10% for the PdO/Al-Nd-10 photocatalyst) is observed after 6 h of irradiation indicating a small presence of no mineralized organic intermediaries.

3.3. Photocatalytic performance

PdO is known to be a *p*-type semiconductor with a band gap not firmly established in the range 0.8–2.67 eV [17]. The valence band is formed by the filled O 2*p* states, which are hybridized with the Pd 4*d* states. The lowest states in the conduction band are associated with the empty Pd 4*d* states. Then, during the photocatalytic processes an electron is promoted from the valence band to the conduction band generating electron/hole pairs by means of irradiation. Smaller band gap energy values indicate an enhanced semiconductive capability. Therefore, it can be inferred that the improvement in the photocatalytic activity of PdO/Al-Nd photocatalysts in the photodegradation of 2,4-D could be due to the decrease in the band gap of the PdO *p*-type semiconductor. However, the lower photocatalytic activity observed in PdO supported on pure Nd_2O_3 suggests that the nature of the support and thereby the chemical state of

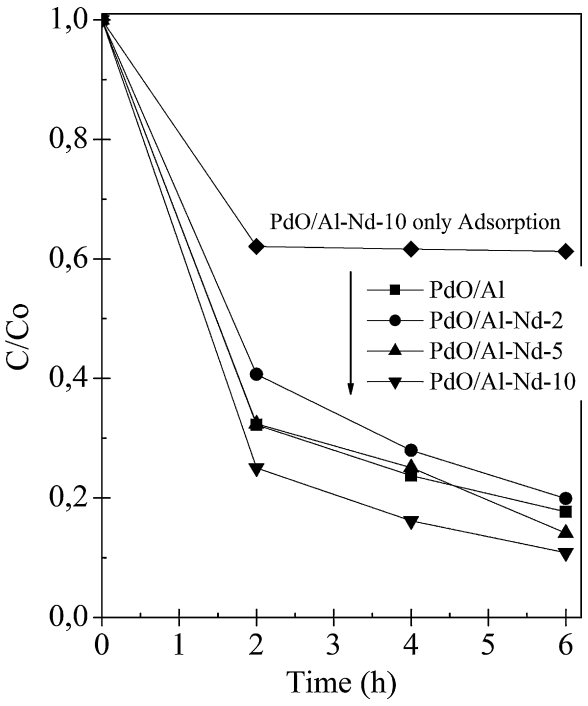

Fig. 10. Total organic carbon (TOC) in the 2,4-D solution as a function of irradiation time on 1 wt% PdO supported on Al_2O_3–Nd_2O_3 binary oxides.

neodymium oxide is crucial in order to promote the improvement in the catalytic activity of PdO/γ-Al_2O_3 catalysts. The lower photocatalytic activity of PdO supported on pure Nd_2O_3 is correlated with its lower S_{BET}, whereas the highest photocatalytic activity observed in the PdO/Al-Nd-10 photocatalyst is due to high S_{BET} of this solid. This observation should imply an increase in dispersion of the PdO conglomerates. Moreover, XRD spectra show that the increase in the Nd_2O_3 concentration in the Al_2O_3–Nd_2O_3 binary oxides arise to a better dispersion of PdO since the intensity of the diffraction peaks of PdO decreases with the increase in the Nd_2O_3 concentration, thus forming smaller PdO particles which could help in the photodegradation processes of 2,4 D by retarding the e^- h^+ recombination.

4. Conclusions

It is showed that PdO/Al_2O_3 catalyst photodegrades the 2,4-D in aqueous solution. The addition of Nd_2O_3 to γ-Al_2O_3 by the sol–gel method notably promotes the photocatalytic activity. As the concentration of Nd_2O_3 in the binary oxide increases to 10 wt%, the photodegradation of 2,4-D as well as the diminution on the total organic carbon is highly enhanced. 2,4-D has been completely destroyed by the PdO/Al_2O_3–Nd_2O_3 photocatalysts after 6 h of UV irradiation.

Acknowledgements

This work was supported partially by grants from CONACYT (Project: 60702), COECYTJAL (Project: 06-2009-732) and PROMEP. The authors thank M. Aguilar Franco for his technical assistance in the XRD measurements.

References

[1] D. Fabbri, A. Crime, M. Davezza, C. Medana, C. Baiocchi, A. Bianco Prevot, E. Pramauro, Appl. Catal. B 92 (2009) 318.
[2] S.U. Khan, Pesticides in the Soil Environment, Elsevier, Amsterdam, 1980.
[3] N. Serpone, E. Pelizzetti, Photocatalysis, Fundamentals and Applications, Wiley, New York, 1989.
[4] D.F. Ollis, H. Al-Ekabi, Photocatalytic Purification of Water and Air, Elsevier, Amsterdam, 1993.
[5] M.R. Hoffman, S.T. Martin, W. Choi, D.W. Bahnemann, Chem. Rev. 95 (1995) 69.
[6] S. Malato, J. Blanco, A. Vidal, C. Richter, Appl. Catal. B 37 (2002) 1.
[7] H.K. Singh, M. Saquib, M.M. Haque, M. Muneer, D.W. Bahnemann, J. Mol. Catal. A: Chem. 264 (2007) 66.
[8] O. Vázquez-Cuchillo, A. Cruz-López, L.M. Bautista-Carrillo, A. Bautista Hernández, L.M. Torres Martínez, S. Wohn Lee, Res. Chem. Intermed. 36 (2010) 103.
[9] U.G. Akpan, B.H. Hameed, Appl. Catal. A 375 (2010) 1.
[10] A.-Ch. Lee, R.-H. Lin, Ch.-Y. Yang, M.-H. Lin, W.-Y. Wang, Mater. Chem. Phys. 109 (2008) 275.
[11] Y. Bessekhouad, D. Robert, J.V. Weber, J. Photochem. Photobiol. A: Chem. 163 (2004) 569.
[12] E. Dvininov, M. Ignat, P. Barvinschi, M.A. Smithers, E. Popovici, J. Hazard. Mater. 177 (2010) 150.
[13] A. Mantilla, F. Tzompantzi, J.L. Fernández, J.A.I. Díaz Góngora, G. Mendoza, R. Gómez, Catal. Today 150 (2010) 353.
[14] A. Mantilla, F. Tzompantzi, J.L. Fernández, J.A.I. Díaz Góngora, G. Mendoza, R. Gómez, Catal. Today 148 (2009) 119.
[15] Y. Guo, D. Li, Ch. Hua, Y. Wang, E. Wang, Y. Zhoub, S. Feng, Appl. Catal. B: Environ. 30 (2001) 337.
[16] P.A. Deshpande, G. Madraz, Chem. Eng. J. 161 (2010) 136.
[17] J.R. McBride, K.C. Hass, W.H. Weber, Phys. Rev. B 44 (10) (1991) 5016.
[18] T.L.R. Hewer, E.C.C. Souza, T.S. Martins, E.N.S. Muccillo, R.S. Freire, J. Mol. Catal. A: Chem. 336 (2011) 58.
[19] Y.H. Xu, C. Chen, X.L. Yang, X. Li, B.F. Wang, Appl. Surf. Sci. 255 (2009) 8624.
[20] B. Shahmoradi, I.A. Ibrahin, N. Sakamoto, S. Ananda, R. Somashekar, T.N. Guru Row, K. Byrappa, J. Environ. Sci. Health A: Toxic/Hazard. Subst. Environ. Eng. 45 (2010) 1248.
[21] D. de la Cruz Romero, G. Torres Torres, J.C. Arévalo, R. Gómez, A. Aguilar-Elguezabal, J. Sol-Gel Sci. Technol. 56 (2010) 219.
[22] C.Y. Kwan, W. Chu, Water Res. 37 (2003) 4405.
[23] D.T. Newby, T.J. Gentry, I.L. Pepper, Appl. Environ. Microbiol. 66 (8) (2000) 3399.
[24] T.S. Muller, Z. Sun, G.M.P. Kumar, K. Itoh, M. Murabayashi, Chemosphere 36 (9) (1998) 2043.
[25] F. Galindo-Hernández, R. Gómez, J. Photoch. Photobiol. A 217 (2011) 383.
[26] R. López, R. Gómez, M.E. Llanos, Catal. Today 148 (2009) 103.
[27] V. Rodríguez-González, M.A. Ruiz-Gómez, L.M. Torres-Martínez, R. Zanella, R. Gómez, Catal. Today 148 (2009) 109.
[28] X. Quan, Q. Zhao, H. Tan, X. Song, F. Wang, Y. Dai, Mater. Chem. Phys. 114 (2009) 90.
[29] V. Rodríguez-González, A. Moreno-Rodríguez, M. May, F. Tzompantzi, R. Gómez, J. Photochem Photobiol. A 193 (2008) 266.
[30] A.N. Pestryakov, V.V. Lunin, S. Fuentes, N. Bogdanchikova, A. Barrera, Chem. Phys. Lett. 367 (2003) 102.
[31] M. Lyubosky, L. Pfefferle, Catal. Today 47 (1997) 29.
[32] F. Oudet, P. Courtine, A. Vejux, J. Catal. 114 (1988) 112.
[33] P. Caro, Structure Electronique des Elements de Transition, Presses Universitaires de France, Paris, 1976.